



1     **Large Ozone Intrusions during Sudden Stratospheric Warmings Enhance**

2                     **Ozone Radiative Forcing over South Asia**

3     Shubhajyoti Roy<sup>1</sup>, Satheesh Chandran PR<sup>1</sup>, Suvarna Fadnavis<sup>1\*</sup>, Vijay Sagar<sup>1</sup>, Michaela I.

4                                     Hegglin<sup>2</sup>, Rolf Müller<sup>2</sup>

5             <sup>1</sup>Centre for Climate Change Research, Indian Institute of Tropical Meteorology, India

6             <sup>2</sup>Institute of Energy and Climate Systems: Stratosphere (ICE-4), Forschungszentrum,

7                                     Jülich, Germany

8                                     \*Corresponding author email: [suvarna@tropmet.res.in](mailto:suvarna@tropmet.res.in)

9

10

11

12

13

14

15

16

17

18

19

20



## 21 Abstract

22 Tropospheric ozone pollution in South Asia is mainly blamed on anthropogenic  
23 emissions. However, this study highlights the contribution of stratospheric ozone  
24 intrusions into the troposphere associated with sudden stratospheric warming (SSW)  
25 events in enhancing tropospheric ozone over the South Asian region using ERA-5  
26 reanalysis data. We report that specifically split-downward propagating SSWs (dSSWs)  
27 cause enormous ozone enhancement in the upper troposphere and lower stratosphere  
28 (UTLS) over South Asia around the dSSW-onset, with a maximum of ~290% within  $\pm 30$   
29 days. The ozone intrusions propagate deep into the troposphere, causing near-surface  
30 maximum ozone increase by 43% within  $\pm 30$  days around the SSW-onset. The ozone  
31 enhancement increases ozone radiative forcing in the troposphere by  $0.04 \pm 0.03 \text{ W.m}^{-2}$   
32 and UTLS by  $0.08 \pm 0.06 \text{ W.m}^{-2}$  over South Asia. Frequent SSW events in a warming  
33 climate will thus likely increase stratospheric ozone intrusions and ozone radiative  
34 forcing over South Asia, potentially exacerbating regional climate warming. The elevated  
35 tropospheric ozone amounts due to stratospheric intrusions are posing threat to humans  
36 and vegetation.

37 Keywords: Sudden stratospheric warming, stratosphere intrusions, ozone radiative  
38 forcing, South Asian region, Rossby wave breaking.

## 39 1. Introduction

40 Tropospheric ozone is a short-lived greenhouse gas that plays a crucial role in  
41 atmospheric chemistry and radiative forcing (Wang et al., 2022). It is also a major air  
42 pollutant that significantly affects human health (Lim et al., 2012; Fleming et al., 2018),  
43 damages vegetation (Fowler et al., 2009; Feng et al., 2021), disrupts ecosystems, and imposes  
44 economic costs (Dewan and Lakhani, 2022). In South Asia, a large amount of tropospheric



45 ozone is a growing concern because of its ill effects, resulting in rising mortality rates (Silva  
46 et al., 2013; Lin et al., 2018).

47       The increase in tropospheric ozone levels in South Asia is primarily attributed to  
48 enhanced anthropogenic emissions (Rathore et al., 2023). However, the contribution from the  
49 downward transport of ozone-rich air from the stratosphere is the largest natural source of  
50 tropospheric ozone. Studies have reported that stratospheric influence on the tropospheric  
51 ozone exceeds 50% in the winter season at the extra tropics (Williams et al., 2019). Wang  
52 and Fu (2021) estimate that stratosphere-to-troposphere exchange (STE) contributes  
53 approximately  $347 \pm 12$  Tg year<sup>-1</sup> to the global tropospheric ozone budget based on both  
54 observations and reanalysis data. CMIP6 models suggest that up to 30% of surface ozone in  
55 the Northern Hemisphere during winter (DJF) is being attributed to stratospheric ozone  
56 intrusions (Li et al., 2024). In the Northwest Pacific, STE increases mid and upper-  
57 tropospheric ozone by about 96% in winter and 40% in summer (Ma et al., 2024). Numerous  
58 observational and reanalysis studies confirm that stratospheric intrusions enhance surface  
59 ozone levels over East Asia and the Tibetan Plateau by ~15 ppb (e.g., Ou-Yang et al., 2022;  
60 Yin et al., 2023). Roy et al. (2023) reported an ozone enhancement of ~40 ppb in the upper  
61 troposphere over the Indian region due to stratospheric intrusions associated with tropical  
62 cyclones.

63       Sudden stratospheric warming (SSW) events are significant drivers of STE, playing a  
64 key role in atmospheric dynamics and stratospheric ozone intrusions into the troposphere  
65 (e.g., Williams et al., 2024). SSWs are one of the most significant large-scale dynamical  
66 phenomena occurring in the stratosphere during winter (Butler et al., 2015; de la Cámara et  
67 al., 2018; Baldwin et al., 2021). Enhanced planetary wave activity from the troposphere  
68 disrupts the stratospheric polar vortex, decelerating or even reversing the stratospheric



69 westerlies, and causing a rapid rise in polar stratospheric temperatures by up to 50 K within  
70 just a few days (Baldwin et al., 2021). SSW events play a crucial role in modulating  
71 tropospheric weather phenomena, such as extreme heat, air pollution, wildfires, wind  
72 extremes, storm clusters, tropical cyclones, and sea ice melt in the northern high latitudes (;  
73 Domeisen and Butler, 2020; Domeisen et al., 2020). The temperature and wind anomalies  
74 associated with SSWs propagate downward into the troposphere over timescales ranging  
75 from weeks to months, impacting surface weather in the Northern Hemisphere for up to 40  
76 days following the event onset (Baldwin and Dunkerton, 2001; Hall et al., 2021). Projection  
77 studies suggest that SSW events will increase by approximately one event per decade by the  
78 end of the 21<sup>st</sup> century (Charlton-Perez et al., 2008), and high greenhouse gas emission  
79 scenarios show a doubling in SSW frequency (Schimanke et al., 2012). Considering the  
80 frequent occurrences and the potential role of SSWs in STE, it is crucial to investigate SSW's  
81 influence on tropospheric ozone enhancements and the associated radiative effects.

82 SSW events are classified into two categories, namely displaced or split events, based  
83 on the geometry of the polar vortex (Charlton and Polvani, 2007). In the displaced case, the  
84 vortex is displaced off the pole, while it is split into two baby vortices in the split case.  
85 Further, SSWs are classified as downward propagating and non-downward propagating.  
86 Downward propagating SSWs (dSSWs) show a downward progression of polar cap height  
87 anomalies across vertical levels that reach the surface and exhibit strong surface impacts,  
88 while this is not the case for non-downward propagating SSWs (nSSWs) (Hall et al., 2021).  
89 dSSWs lead to long-lasting tropospheric circulation changes in contrast to nSSWs (;  
90 Karpechko et al., 2017). The dSSWs are often followed by an equatorward shift of the  
91 tropospheric jet stream and storm tracks, as well as surface pressure anomalies that resemble  
92 the negative phase of the Northern Annular Mode (Sigmond et al., 2013; Kidston et al.,  
93 2015). Among dSSWs, studies indicate that the surface effects of split events typically appear



94 nearly a week earlier than those of displaced SSWs (Mitchell et al., 2013; Hall et al., 2021).  
95 Furthermore, CMIP5 models suggest that split events tend to propagate downward to the  
96 surface more quickly than displacement events (Hall et al., 2021).

97 SSW events significantly influence STE and impact the tropospheric ozone budget,  
98 particularly in high-latitude regions (Xia et al., 2023; Lu et al., 2023; Williams et al., 2024).  
99 Based on SSW events from 1980–2013 and chemistry-climate model simulations, STE led to  
100 an average 5–10% increase in near-surface ozone over the Arctic (Williams et al., 2024). Xia  
101 et al. (2023) reported an even more pronounced increase of 76% in Arctic surface ozone due  
102 to STE in the 2020/21 SSW event. While most of these studies focus on the polar regions,  
103 some have identified SSW-induced ozone variability in the mid-latitudes as well (Liu et al.,  
104 2009; Lu et al., 2022; Williams et al., 2024). For example, Lu et al. (2022) demonstrated that  
105 meteorological changes associated with SSWs cause poor air quality in the Beijing-Tianjin-  
106 Hebei region. Liu et al. (2009) noted an ozone enhancement of about 186 Tg in the upper  
107 troposphere over East Asia during the 2002–2003 SSW, using MOZART-3 simulations.  
108 However, tropospheric ozone variations during SSW events over South Asia are among the  
109 least studied. Additionally, the broader implications of these events on the ozone radiative  
110 forcing over this region remain largely underexplored. In this study, we investigate the  
111 impact of all the downward-propagating SSW events from 1962 to 2018 on tropospheric  
112 ozone variability over South Asia [20–35°N, 65–90°E] using ERA5 data. The composite is  
113 obtained by averaging data with the onset day as a central date (details in the ‘Methods’  
114 section). Here, we report enormous ozone enhancement in the troposphere over South Asia,  
115 leading to an increase in ozone radiative forcing, which further elevates warming in South  
116 Asia. We present a detailed mechanism for the latest 2018 split-dSSW event and a composite  
117 analysis of all split-dSSW events from 1962 to 2018. The net radiative forcing estimation  
118 using the radiative kernel approach is described in the ‘Methods’ section.



## 119    **2. Methods**

### 120    **2.1 ERA 5 Data**

121            We analysed daily data of ozone, zonal and meridional winds, geopotential height,  
122    and potential vorticity (PV) from the fifth-generation reanalysis dataset (ERA5) provided by  
123    the European Centre for Medium-Range Weather Forecasts (ECMWF) (Hersbach et al.,  
124    2020). The ERA5 data, with a horizontal resolution of  $0.25^\circ \times 0.25^\circ$  and 37 pressure levels  
125    ranging from 1000 hPa to 1 hPa, were utilized for this study. Composite analysis was  
126    conducted for all variables for a 121-day period centred on the onset of SSW events (60 days  
127    before and after the onset) to assess the impact. Daily anomalies in ozone, geopotential  
128    height, winds, and PV during the SSW days were calculated by subtracting the corresponding  
129    daily mean of all the non-SSW days for  $\pm 61$  days near the onset of the SSW. The anomalies  
130    obtained from climatology (1962-2018) also show features similar to those when one use the  
131    mean of all the non-SSW days (see Fig. S1. and Fig. 1a-b). We prefer to use the mean of all  
132    the non-SSW days instead of climatology since climatology includes SSW events.

133            The onset of each SSW event is identified as the day when the zonal mean westerly  
134    winds at 10 hPa and  $60^\circ\text{N}$  reverse their direction from westerlies to easterlies (Charlton and  
135    Polvani 2007). Figure S2. shows the temporal evolutions of the zonal-mean zonal wind at  $60^\circ$   
136    N and 10 hPa for all the split-dSSWs considered for the present study.

### 137    **2.2 Computation of ozone radiative forcing**

138            The radiative forcing (RF) due to ozone is estimated using an ozone radiative kernel  
139    method (Skeie et al 2020). The radiative kernel is constructed using the University of Oslo  
140    radiative transfer model (Myhre et al., 2011) by perturbing the ozone layer by layer.  
141    Temperature, water vapour, and clouds are incorporated into the model from ECMWF's



142 forecast for the year 2003 and applied as monthly averages. The model calculates radiative  
143 forcing using a broad-band scheme for longwave (Myhre and Stordal, 1997) and DIScrete  
144 Ordinate Radiative Transfer code for shortwave (Stamnes et al., 1988). Previous studies show  
145 that the ozone radiative forcing estimates from the radiative-kernel technique and radiative  
146 transfer model agree within  $0.01 \text{ W.m}^{-2}$  globally (Iglesias-Suarez et al., 2018). Before the  
147 application of kernel, the ERA5 ozone data is linearly interpolated to the kernel resolution  
148 ( $\sim 5.6^\circ \times 5.6^\circ$  horizontal with 60 vertical levels). This interpolated ozone field is converted  
149 into Dobson units following Ziemke et al. (2001) and is multiplied with the kernel to estimate  
150 the RF. The tropospheric ozone RF is determined by summing the RF contributions from all  
151 atmospheric layers between the surface and the tropopause (Shell et al., 2008). A similar  
152 approach is applied to estimate radiative forcing for the UTLS region and the total  
153 atmosphere. The tropopause pressure is identified based on the WMO lapse rate tropopause  
154 definition.

### 155 **2.3 Dynamical changes in PV, GPH and ozone in the stratosphere during the 2018 event**

156 The time evolution of the vortex structure depicted by PV at 10 hPa for  $\pm 60$  days  
157 around the 2018 SSW onset is shown in Fig. S3. Since SSW effects are seen for  $\pm 60$  days  
158 around the onset (Limpasuvan et al., 2004; Scheffler et al., 2022), we analysed the evolution  
159 of SSW during these days. As the SSW event approaches, the vortex begins to elongate and  
160 become asymmetrical due to the influence of planetary waves propagating upward from the  
161 troposphere, such deformation of vortex is reported in the past (e.g., Baldwin et al., 2021).  
162 Sixty days before onset, a strong, stable polar vortex is evident, but as the event approaches,  
163 planetary wave activity causes elongation and asymmetry (Fig. S3). On the onset day (12  
164 February), the vortex splits into two high-PV lobes over Eurasia and North America (Fig.  
165 S3h). Following the onset, baby vortices exhibit swirling and filamentation, with the Eurasian



166 lobe drifting westward. Earlier, de la Camara et al. (2018) demonstrated that planetary-scale  
167 wave breaking intensifies mixing and facilitates the diffusion of PV from the vortex by  
168 elongating and stirring the PV fields. These PV variations align with changes in GPH and  
169 ozone fields (e.g., Baldwin et al., 2021), emphasizing stratospheric circulation changes (Fig.  
170 S3).

171        Since major changes in the vortex occur  $\pm 6$  days around the onset, we show the  
172 variations in ozone and GPH during this period (Fig. S4). The GPH anomalies at 10 hPa  
173 highlight stratospheric circulation changes, showing a transition from a wave-1 to a wave-2  
174 pattern just before onset. On onset day, strong positive GPH anomalies appear over the  
175 Arctic, while negative anomalies correspond to the baby vortices (Fig. S4a-h). This pattern  
176 persists for six days and weakens as positive anomalies extend into the United States. Ozone  
177 anomalies follow a similar pattern (Fig. S4i-p), with negative values inside the vortex during  
178 the pre-onset period due to chemical loss (Manney et al., 2015; Baldwin et al., 2021). After  
179 onset, the transport of ozone-rich air leads to positive anomalies at the North Pole. A similar  
180 sudden increase in the transport of ozone-rich and high GPH air to the polar region on the  
181 onset days is reported by many other studies (Bouillon et al., 2023; Veenus et al., 2023; Shi et  
182 al., 2024). Following the onset, positive ozone anomalies spread southward along two  
183 branches, one along the northern parts of Africa, Eurasia and the Indian subcontinent and the  
184 other over the Atlantic and southern US. This indicates the transport of ozone-rich air  
185 towards lower latitudes. Several studies have reported earlier that SSWs cause stratosphere-  
186 troposphere coupling in the mid and low latitudes (e.g., Gomez-Escolar et al., 2014; Albers et  
187 al., 2016; Williams et al., 2024). The disruption of the polar vortex and the resulting  
188 stratospheric conditions redirect planetary waves toward lower latitudes, leading to  
189 significant tropospheric circulation changes (Gomez-Escolar et al., 2014).



### 190 3. Results

#### 191 3.1 Vertical variation of Ozone over the South Asian region during SSW events

192 We investigated all SSW events from 1962 to 2018 to assess their impact on ozone  
193 variability in the upper troposphere over the South Asian region. The categorization of  
194 split/displaced and downward (dSSW)/non-downward (nSSW) propagating SSW is as per  
195 Hall et al., (2021). Table 1 lists the split-dSSW, displaced-dSSW, and nSSW events  
196 considered in this study.

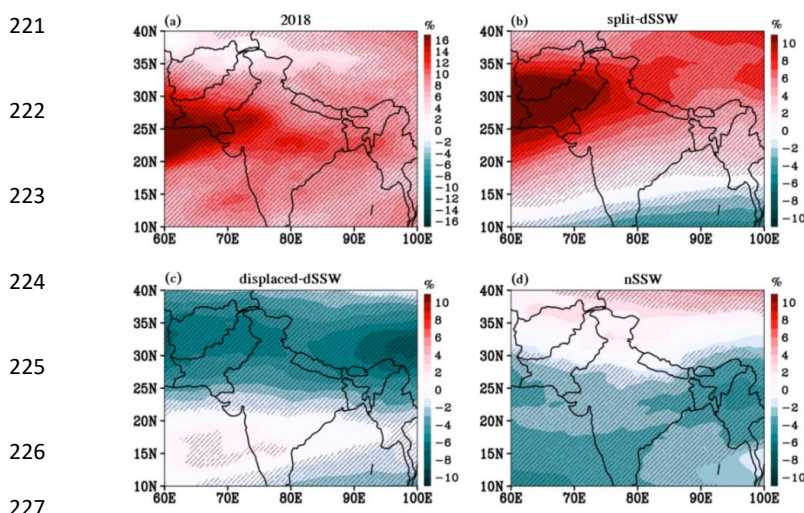
197 **Table 1.** List of downward propagating split SSW events from 1962 to 2018 considered for  
198 the present analysis alongside their onset dates.

Split dSSW	Onset day	Displaced dSSW	Onset day	non- downward SSW	Onset day
1963	28 January	1965	16 December	1966	23 February
1968	7 January	1968	28 November	1969	13 March
1971	20 March	1980	29 February	1970	2 January
1977	9 January	1981	4 March	1971	18 January
1979	22 February	1981	4 December	1973	31 January
1985	1 January	1984	24 February	1987	23 January
1988	14 March	1998	15 December	1987	8 December
1999	26 February	2000	20 March	1989	21 February
2009	24 January	2001	11 February	2001	30 December
2010	9 February	2004	5 January	2003	18 January
2013	6 January	2006	21 January	2007	24 February
2018	12 February	2008	22 February		
		2010	24 March		

206 We analyzed ozone variations in the UTLS during split-dSSW, displaced-dSSW, and  
207 nSSW events. During the SSW event, the disrupted vortex couple with the troposphere,  
208 causing shifts in the tropospheric westerly jet and distinctive patterns of anomalous surface  
209 temperature and sea-level pressure over a period up to 60 days after SSW onset (e.g.,  
210 Mitchell et al., 2013; Butler et al., 2017). Figure 1a-d illustrates spatial maps of ozone



211 anomalies in the UTLS over the South Asian region, averaged over 30 days prior to and after  
212 SSW onset ( $\pm 30$  days) for the aforementioned cases. There is a distinct enhancement in ozone  
213 levels in the UTLS, in the  $20^{\circ}$ – $35^{\circ}$ N belt, by 8–16% (40 – 45 ppbv) in the 2018 split-dSSW  
214 event and by 4–10% (35 – 40 ppbv) in the composite of all split-dSSWs compared to the non-  
215 SSW climatology (Fig. 1a-1b). Ozone enhancement in the UTLS is not seen for  $\pm 30$  days in  
216 the case of displaced-dSSW and nSSW events (see Fig. 1c-d). This highlights the importance  
217 of considering split-dSSW events when assessing the impact of SSWs on ozone variability in  
218 the South Asian region. Ozone enhancement is associated with Rossby wave breaking  
219 (RWB) in the vicinity of the South Asian region which is seen only in the case of split-dSSW  
220 (discussed in section 2.2).



228 **Figure 1.** Composite map of ERA5 ozone anomalies in the UTLS (250–50 hPa) over the  
229 South Asian region, averaged from  $\pm 30$  days around the onset for (a) the 2018 split-dSSW  
230 event, (b) all split-dSSWs (12 events), (c) all displaced-dSSWs (12 events), and (d) all  
231 nSSWs (9 events) as listed in Table-1. Hatched lines in Figs. a-d indicates a region of 95%  
232 confidence level based on the student's t-test. (Figure created using the COLA/GrADS  
233 software).

234 Figures 2a-b show the temporal evolution of vertical ozone anomalies averaged over  
235 South Asia for the 2018 split-dSSW event and the composite of all split-dSSWs. There is a



236 large ozone enhancement in the UTLS, with values  $>80\%$  ( $>150$  ppb) in 2018 and  $>30\%$   
237 ( $>80$  ppb) for the composite of split-dSSWs within  $\pm 6$  days around the SSW-onset. Figure  
238 2a-b indicates that the ozone enhancements in the UTLS region are episodic and coincide  
239 with downward propagating negative geopotential height (GPH) anomalies. The negative  
240 GPH anomaly and lowering of the 380 K potential temperature isoline along with a positive  
241 ozone enhancement in Fig. 2a-b indicate stratospheric intrusions associated with SSW events.  
242 The ozone intrusions over the Indian region are stronger from 5 days before the onset and last  
243 for  $\sim 15$  days, causing an ozone enhancement of  $\sim 36\%$  in 2018 and 16 % in split-DSSW  
244 composite in the UTLS during this period (see Fig. S5a-b).

245 Figure 2 a-b shows that ozone enhancement in the UTLS is smaller in composite split-  
246 dSSW than in 2018 (in the UTLS, and surface). This subdued effect is due to averaging  
247 across multiple episodic events occurring at different times within  $\pm 30$  days around the SSW  
248 onset. Hence, to show the ozone enhancement during the SSW event, we picked up the  
249 maximum ozone increase within  $\pm 30$  days in the upper troposphere and near the surface over  
250 South Asia for each of the split dSSWs (Fig. 2c-d). Figure 2c-d shows clear evidence of a  
251 substantial ozone increase (50 to 250 %) in the UTLS (150 hPa) and (15 to 45%) near the  
252 surface (850 hPa) during the split-dSSWs. Further, the lead-lag correlation between the ozone  
253 variation in the upper troposphere and at surface levels shows that downward propagation of  
254 ozone from 200 hPa to the near-surface occurs with 10- and 25-days lag in 2018 and 5- days  
255 lead to 10- days lag in the case of composite (Fig. S6).

256

257

258

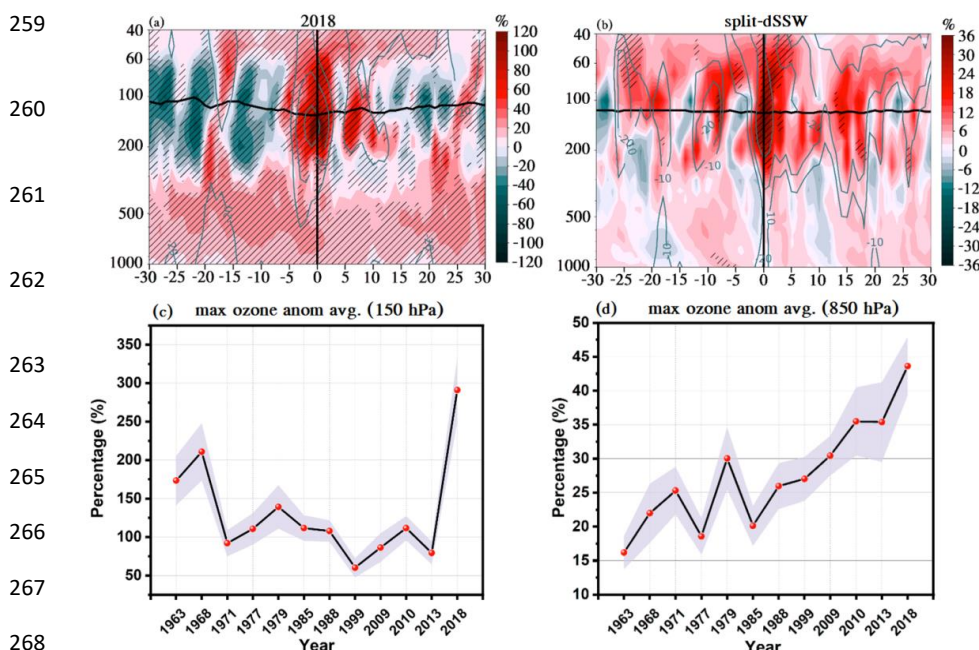


**Figure 2.** Temporal evolution of vertical ozone anomalies averaged over the South Asian region (65-90°E, 20-35°N) from 30 days before to 30 days after the onset for (a) the 2018 split dSSW event and (b) all the split dSSWs. Hatched lines in Figs. a-b indicates a region of 95% confidence level based on the student's t-test. The sky blue contour line represents the GPH anomaly during the respective period. The horizontal solid line represents 380 K potential temperature isoline, and the vertical solid line represents the onset day. Average of the daily maximum ozone increase within  $\pm 30$  days over South Asia for each of the split dSSWs in the (c) upper troposphere (150 hPa) and (d) near-surface (850 hPa). The shading in (c) and (d) represents standard error. (Figure created using the COLA/GrADS software).

The latitude-pressure (Fig. 3a-b) and longitude-pressure (Fig. 3c-d) cross-sections of ozone anomalies show large ozone enhancement for  $\pm 6$  days around the onset in the UTLS over South Asia exceeding  $>60\%$  in 2018 and  $>20\%$  in the composite of split-dSSW events. Interestingly, a peak in ozone enhancement is seen at the subtropical jet core (Fig. 3a-b). This suggests the role of the subtropical jet causing ozone enhancement in the upper troposphere over South Asia (discussed later in this section). The anomalous lowering of the tropopause levels along with a strong negative GPH anomaly (indicating a low-pressure area) coincident with large ozone enhancements, provides evidence of stratospheric intrusions occurring during these split-dSSWs (Fig. 3c-d). Past literature reports ozone enhancements in



the polar region associated with dSSWs (e.g., Baldwin et al., 2021); however, high ozone enhancement in the UTLS over the South Asian region underscores the unique regional impacts of split-dSSWs.

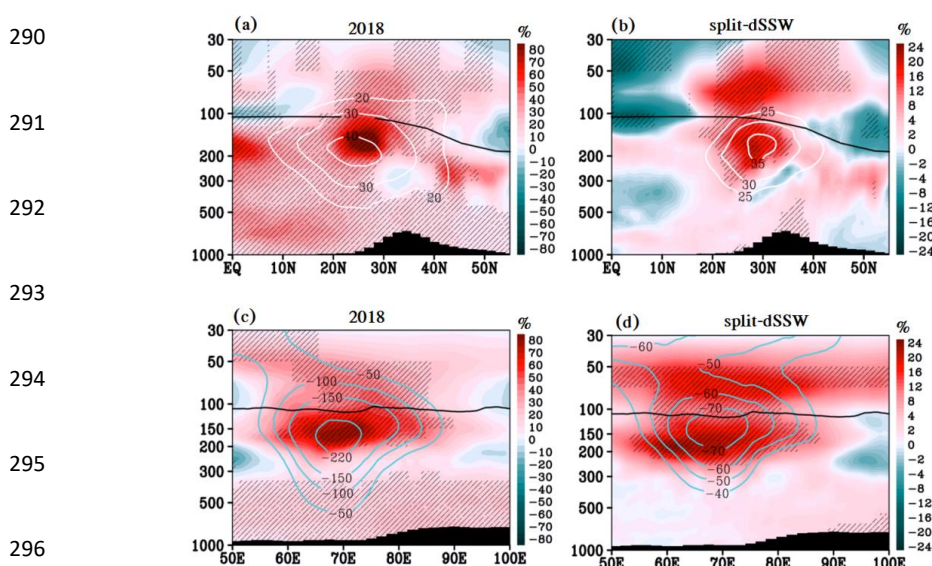


**Figure 3.** Latitude-pressure section of ozone anomalies averaged over South Asia (65 - 90°E) for  $\pm 6$  days around the split-dSSW onset for (a) the 2018 event, and (b) the composite of all the split-dSSWs. Figures (c) and (d) are the same as those of (a) and (b) but represent longitude variations of vertical ozone anomalies averaged over South Asia (20-35°N). White contour lines in (a) and (b) represent the mean zonal wind, and sky blue contour lines in (c) and (d) represent the GPH anomaly. Solid black lines in panels a-d represent the tropopause. Hatched lines in panels a-d indicate a region of 95% confidence level based on the student's t-test (Figure created using the COLA/GrADS software).

### 3.2 Changes in upper tropospheric dynamics and Rossby wave activities associated with the 2018 dSSW event

In this section, we discuss the possible mechanism responsible for the ozone enhancement in the UTLS over South Asia associated with the 2018 dSSW event. The dynamic changes happening in the vortex for 2018 are discussed in the section 2. For the 2018 SSW, the vortex starts deforming 6 days before the SSW-onset and splits on 12 February 2018. After the vortex split, two baby vortices are seen centred over Eurasia and



312 North America for 6 days after the onset. Although the vortex over North America remains  
313 anchored in that location, the vortex centred over Eurasia gradually drifts westward toward  
314 the North Atlantic during this period (see section 2).

315 Several studies have shown that SSW-related planetary wave disturbances occur  
316 across a deep layer of the stratosphere (e.g., McIntyre, 1982; McIntyre and Palmer, 1983;  
317 Albers et al., 2016). These disturbances, which are strong in the mid-to-upper stratosphere,  
318 extend downward and disrupt horizontal flows in the upper troposphere (200 hPa) (Albers et  
319 al., 2016). We analyzed GPH anomalies at 10 hPa and 200 hPa to understand the coupling  
320 between the stratosphere and the upper troposphere. Figure 4 illustrates the evolution of GPH  
321 anomalies at 10 hPa and 200 hPa, and ozone anomalies at 200 hPa for  $\pm 6$  days around the  
322 SSW onset (Feb 12, 2018). Our analysis shows strong vertical coherence between 10 and 200  
323 hPa levels (see Fig. 4a–e and Fig. 4f–j). Interestingly, the GPH anomalies at 10 hPa and 200  
324 hPa north of 40°N show patterns of wave-1 and wave-2 with lows over America and Eurasia  
325 for  $\pm 6$  days around the onset. The SSW event thus affects the upper tropospheric subtropical  
326 jet, which peaks at 200 hPa (Albers et al., 2016).

327 When the polar vortex splits and the baby vortices move towards the mid-latitudes,  
328 they push the mid-latitude synoptic-scale waveguide structure farther equatorward. This  
329 displacement channels the eastward propagating synoptic-scale Rossby waves toward the  
330 Indian Ocean region, where they eventually break (Albers et al., 2016). The pattern of high  
331 and low GPH anomalies in the subtropical region (15–40°N) seen in Fig. 4f–j shows synoptic-  
332 scale Rossby waves occurring in the upper troposphere. Rossby wave breaking (RWB) is  
333 seen as large filaments of high-PV air extending towards the equator. Such intrusions extend  
334 downward from the lower stratosphere into the upper troposphere, causing an enhancement in  
335 ozone (e.g. Holton et al., 1995; Waugh and Polvani, 2000; Albers et al., 2016). The 2 PVU



contour lines and ozone anomaly maps at 200 hPa depicted in Fig. 4k-o show clear indications of ozone intrusions penetrating deep into the tropics, particularly over South Asia. The persistent low and high GPH anomaly over South Asia indicates a deepening trough associated with the eastward propagation of Rossby waves, facilitating enhanced stratospheric intrusions (Figs. 4f-j).

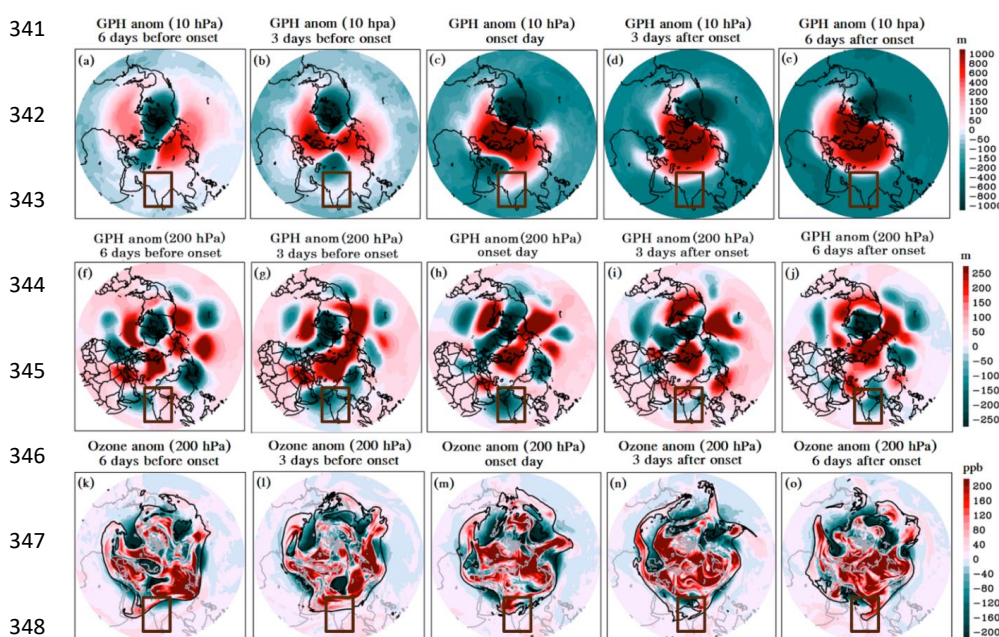


**Figure 4.** Spatial map of (a-e) GPH anomaly at 10 hPa, (f-j) GPH anomaly at 200 hPa, and (k-o) ozone anomaly at 200 hPa from 6 days before to 6 days after the onset of the 2018 split-dSSW event, shown at 3-day intervals. The black solid line in panels (k-o) represents the 2 PVU isoline. The square box represents the South Asian region considered for the present study (Figure created using the COLA/GrADS software).

RWB facilitates the stripping of stratospheric air (indicated by the 2 PVU contour) along the eastern flank of an anticyclonic centre (positive GPH anomaly, Fig. 4f-j) over the South Asian region, causing large ozone enhancements (Fig. 4k-o). Figures 4k-o clearly show that these episodic intrusions cause large ozone enhancements >150 ppb (>80%) over South Asia. The time evolution of zonal winds depicted in Figure 5a-b also shows that thirty



359 days before the onset, the subtropical jet core is positioned over the northern part of the  
360 Indian subcontinent but migrates equatorward near the onset day (Fig. 5a). The vertical  
361 variation of zonal wind clearly depicts the intensification of westerly wind over the Indian  
362 region around 200 hPa close to the onset day, facilitating Rossby wave intrusions (Fig. 5b).  
363 The strength of zonal wind is strong within  $\pm 6$  days around the onset, causing higher ozone  
364 intrusions during this period (see Figs. 2a-b and Fig. 5b). Earlier, Albers et al. (2016) have  
365 shown that the PV intrusion associated with split SSWs has a significant contribution over the  
366 Indian Ocean. Further, we analysed the synoptic wave structure prevailing in the upper  
367 troposphere for different SSW cases viz. split-dSSW, split-nSSW, displaced-dSSW, and  
368 displaced-nSSW (Figures 5c-f). Figure 5c clearly shows that the persistence of synoptic wave  
369 structures is prominent only in the split-dSSW cases. It is not evident in other SSW types  
370 (Fig. 5d-f). This persistence of synoptic wave structures enhances RWBs, causing large  
371 ozone intrusions during the split-dSSW events.

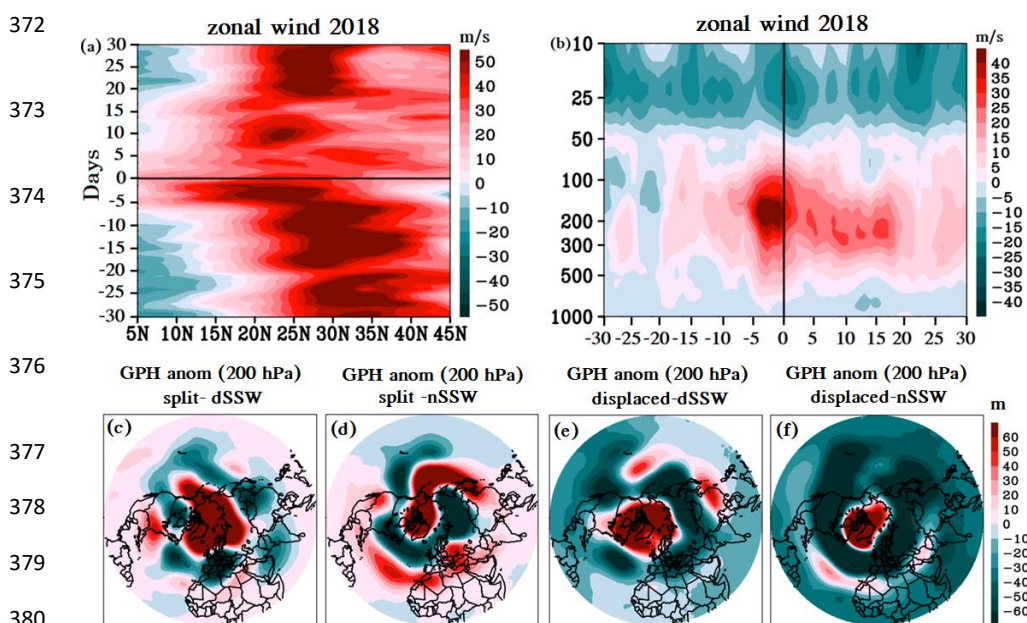
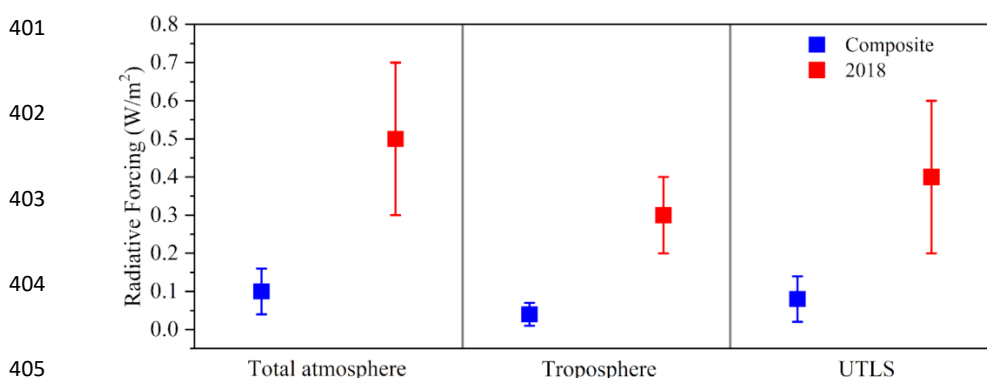




**Figure 5.** (a) Latitude-time plot of zonal wind averaged over South Asia ( $65^{\circ}$  to  $90^{\circ}$  E). (b) Temporal evolution of vertical zonal wind averaged over the South Asian region ( $65^{\circ}$  -  $90^{\circ}$  E,  $10^{\circ}$  -  $20^{\circ}$  N) for  $\pm 30$  days around the onset of the 2018 dSSW event. The horizontal (in Fig. a) and vertical (in Fig. b) solid lines in the figure represent the onset day. Composite map of GPH anomaly at 200 hPa averaged for  $\pm 6$  days around the onset during (c) split-dSSW, (d) split-nSSW, (e) displaced-dSSW, and (f) displaced-nSSW cases. (Figure created using the COLA/GrADS software).

### 3.3 Radiative impact of ozone associated with split-dSSW over the South Asian region

Further, we assessed the radiative impact of ozone enhancements in the UTLS and troposphere over the South Asian region associated with split-dSSW events. Figure 6 presents the computed radiative forcing of ozone averaged over the South Asian region for the 2018 split-dSSW event and the composite of all downward propagating split-dSSWs for  $\pm 6$  days around the onset. In the troposphere, a positive radiative forcing of  $0.3 \pm 0.1 \text{ W.m}^{-2}$  is observed in the 2018 split-dSSW event, while the composite exhibits a forcing of  $0.04 \pm 0.03 \text{ W.m}^{-2}$  (Fig. 6). In contrast, the UTLS, where the largest percentage increases in ozone are observed, shows a radiative forcing of  $0.4 \pm 0.2 \text{ W.m}^{-2}$  for the 2018 event and  $0.08 \pm 0.06 \text{ W.m}^{-2}$  for the composite. For the total atmosphere, the ozone radiative forcing is  $0.5 \pm 0.2 \text{ W.m}^{-2}$  for the 2018 event and  $0.1 \pm 0.06 \text{ W.m}^{-2}$  for the composite. These results highlight the significant role of split-dSSW events in modulating the radiative balance in the troposphere, particularly in the UTLS over South Asia.





406 **Figure 6.** Average ozone radiative forcing ( $\text{W.m}^{-2}$ ) in the total atmosphere, troposphere, and  
407 UTLS over the South Asian region calculated for the  $\pm 6$  days around the onset of the 2018  
408 SSW event and all split dSSW composites (Figure created using Origin, OriginLab,  
409 Northampton, MA).

#### 410 **4. Conclusions**

411 The ERA5 reanalysis data shows Rossby wave intensification during split-dSSWs  
412 observed for the 1962-2018 time period, which lead to upper tropospheric intrusions over the  
413 South Asian region. This leads to substantial ozone enhancements over South Asia, with  
414 maximum increases of  $\sim 290\%$  and an average of  $130\%$  in the UTLS region, and surface-level  
415 enhancements reaching up to  $43\%$ , with an average increase of  $27\%$  (see Fig. 2c-d). The  
416 ozone enhancement due to split-dSSWs events is episodic, however, impacts are observed for  
417  $\sim 2$  months around the SSW onset date.

418 Near surface ozone enhancements over South Asia also result from factors other than  
419 SSW events, including (1) anthropogenic emissions, which increase surface ozone by  $20\text{--}30$   
420 ppb over this region (Gao et al., 2020), and (2) biomass burning that is prominent in the  
421 winter and pre-monsoon period causing a surface ozone increase by  $\sim 5\text{--}10$  ppb (Gao et al.,  
422 2020). However, ozone enhancements during split-dSSW are substantial over South Asia,  
423 leading to an increase in tropospheric ozone radiative forcing of  $0.04 \pm 0.03 \text{ W.m}^{-2}$  and in  
424 the UTLS by  $0.08 \pm 0.06 \text{ W.m}^{-2}$  for the composite of all the split-dSSWs, in comparison,  
425 changes in anthropogenic emissions over South Asia contribute to a tropospheric ozone  
426 radiative impact by  $0.02\text{--}0.04 \text{ W.m}^{-2}$  for 2013–2017 relative to 1995–1999 (Wang et al.,  
427 2022). These findings underscore the critical role of split-dSSWs in modulating radiative  
428 forcing, highlighting their importance as natural drivers of climate variability in addition to  
429 anthropogenic influences.



430           This large increase in radiative forcing produces positive feedback on the warming  
431 climate of this region. The ozone intrusions are warranted to elevate pollution effects and  
432 climate warming, impacting people's health, the ecosystem, and the economy. It is projected  
433 that the frequency of SSWs will increase in a warming climate, which will further increase  
434 stratospheric ozone intrusions and potentially amplify the consequences of positive feedback  
435 mechanisms. Hence, we emphasise that climate model should be extended to the stratosphere  
436 including polar vortex dynamics for accurate prediction of climate over South Asia. The  
437 increase in ozone levels due to biomass burning and anthropogenic activities in South Asia  
438 during the winter and pre-monsoon seasons, combined with ozone enhancement from SSW  
439 events, will exacerbate ozone pollution across the region. Since SSWs cause large increase in  
440 tropospheric ozone over South Asia it should be considered as one of the predictors while  
441 prediction of pollution.

442

#### 443 **Code and data availability**

444 The code and data used in this paper are available from <https://zenodo.org/uploads/14604205>

#### 445 **Author contributions**

446 Conceptualisation: S.F. Supervision: SF, MH, PH, RF Investigation and methodology: SC,  
447 SR and VS. Writing: all authors.

#### 448 **Competing interests**

449 At least one of the (co-)authors is a member of the editorial board of Atmospheric Chemistry  
450 and Physics.

451

452

453

454



455 **References:**

- 456 Albers, J. R., Kiladis, G. N., Birner, T. and Dias, J.: Tropical upper-tropospheric potential  
457 vorticity intrusions during sudden stratospheric warmings, *Journal of the Atmospheric*  
458 *Sciences*, 73(6), 2361–2384, doi:10.1175/jas-d-15-0238.1, 2016.
- 459 Baldwin, M. P. and Dunkerton, T. J.: Stratospheric harbingers of anomalous weather  
460 regimes, *Science*, 294(5542), 581–584, doi:10.1126/science.1063315, 2001.
- 461 Bouillon, M., Safieddine, S. and Clerbaux, C.: Sudden stratospheric warmings in the  
462 northern hemisphere observed with Iasi, *Journal of Geophysical Research: Atmospheres*,  
463 128(17), doi:10.1029/2023jd038692, 2023.
- 464 Butler, A. H., Seidel, D. J., Hardiman, S. C., Butchart, N., Birner, T. and Match, A.:  
465 Defining sudden stratospheric warmings, *Bulletin of the American Meteorological*  
466 *Society*, 96(11), 1913–1928, doi:10.1175/bams-d-13-00173.1, 2015.
- 467 Butler, A. H., Sjöberg, J. P., Seidel, D. J. and Rosenlof, K. H.: A sudden stratospheric  
468 warming compendium, *Earth System Science Data*, 9(1), 63–76, doi:10.5194/essd-9-63-  
469 2017, 2017.
- 470 Charlton, A. J. and Polvani, L. M.: A new look at stratospheric sudden warmings. part I:  
471 Climatology and modeling benchmarks, *Journal of Climate*, 20(3), 449–469,  
472 doi:10.1175/jcli3996.1, 2007.
- 473 Charlton-Perez, A. J., Polvani, L. M., Austin, J. and Li, F.: The frequency and dynamics  
474 of stratospheric sudden warmings in the 21st century, *Journal of Geophysical Research:*  
475 *Atmospheres*, 113(D16), doi:10.1029/2007jd009571, 2008.



- 476 Dewan, S. and Lakhani, A.: Tropospheric ozone and its natural precursors impacted by  
477 climatic changes in emission and dynamics, *Frontiers in Environmental Science*, 10,  
478 doi:10.3389/fenvs.2022.1007942, 2022.
- 479 de la Cámara, A., Abalos, M. and Hitchcock, P.: Changes in stratospheric transport and  
480 mixing during sudden stratospheric warmings, *Journal of Geophysical Research:*  
481 *Atmospheres*, 123(7), 3356–3373, doi:10.1002/2017jd028007, 2018.
- 482 Domeisen, D. I. and Butler, A. H.: Stratospheric drivers of extreme events at the Earth’s  
483 surface, *Communications Earth & Environment*, 1(1), doi:10.1038/s43247-020-  
484 00060-z, 2020.
- 485 Domeisen, D. I., Grams, C. M. and Papritz, L.: The role of North Atlantic–European  
486 weather regimes in the surface impact of sudden stratospheric warming events, *Weather*  
487 *and Climate Dynamics*, 1(2), 373–388, doi:10.5194/wcd-1-373-2020, 2020.
- 488 Feng, Z., Agathokleous, E., Yue, X., Oksanen, E., Paoletti, E., Sase, H., Gandin, A.,  
489 Koike, T., Calatayud, V., Yuan, X., Liu, X., De Marco, A., Jolivet, Y., Kontunen-  
490 Soppela, S., Hoshika, Y., Saji, H., Li, P., Li, Z., Watanabe, M. and Kobayashi, K.:  
491 Emerging challenges of ozone impacts on Asian plants: Actions are needed to protect  
492 ecosystem health, *Ecosystem Health and Sustainability*, 7(1),  
493 doi:10.1080/20964129.2021.1911602, 2021.
- 494 Fleming, Z. L., Doherty, R. M., von Schneidmesser, E., Malley, C. S., Cooper, O. R.,  
495 Pinto, J. P., Colette, A., Xu, X., Simpson, D., Schultz, M. G., Lefohn, A. S., Hamad, S.,  
496 Moolla, R., Solberg, S. and Feng, Z.: Tropospheric Ozone Assessment Report: Present-  
497 day ozone distribution and trends relevant to human health, *Elementa: Science of the*  
498 *Anthropocene*, 6, doi:10.1525/elementa.273, 2018.



- 499 Fowler, D., Pilegaard, K., Sutton, M. A., Ambus, P., Raivonen, M., Duyzer, J., Simpson,  
500 D., Fagerli, H., Fuzzi, S., Schjoerring, J. K., Granier, C., Neftel, A., Isaksen, I. S. A., Laj,  
501 P., Maione, M., Monks, P. S., Burkhardt, J., Daemmgen, U., Neirynck, J., Personne, E.,  
502 Wichink-Kruit, R., Butterbach-Bahl, K., Flechard, C., Tuovinen, J. P., Coyle, M., Gerosa,  
503 G., Loubet, B., Altimir, N., Gruenhage, L., Ammann, C., Cieslik, S., Paoletti, E.,  
504 Mikkelsen, T. N., Ro-Poulsen, H., Cellier, P., Cape, J. N., Horváth, L., Loreto, F.,  
505 Niinemets, Palmer, P. I., Rinne, J., Misztal, P., Nemitz, E., Nilsson, D., Pryor, S.,  
506 Gallagher, M. W., Vesala, T., Skiba, U., Brüggemann, N., Zechmeister-Boltenstern, S.,  
507 Williams, J., O'Dowd, C., Facchini, M. C., de Leeuw, G., Flossman, A., Chaumerliac, N.  
508 and Erisman, J. W.: Atmospheric composition change: Ecosystems–atmosphere  
509 interactions, *Atmospheric Environment*, 43(33), 5193–5267,  
510 doi:10.1016/j.atmosenv.2009.07.068, 2009.
- 511 Gao, M., Gao, J., Zhu, B., Kumar, R., Lu, X., Song, S., Zhang, Y., Jia, B., Wang, P.,  
512 Beig, G., Hu, J., Ying, Q., Zhang, H., Sherman, P. and McElroy, M. B.: Ozone pollution  
513 over China and India: Seasonality and sources, *Atmospheric Chemistry and Physics*,  
514 20(7), 4399–4414, doi:10.5194/acp-20-4399-2020, 2020.
- 515 Gómez-Escolar, M., Calvo, N., Barriopedro, D. and Fueglistaler, S.: Tropical response to  
516 stratospheric sudden warmings and its modulation by the QBO, *Journal of Geophysical*  
517 *Research: Atmospheres*, 119(12), 7382–7395, doi:10.1002/2013jd020560, 2014.
- 518 Hall, R. J., Mitchell, D. M., Seviour, W. J. and Wright, C. J.: Tracking the stratosphere-  
519 to-surface impact of sudden stratospheric warmings, *Journal of Geophysical Research:*  
520 *Atmospheres*, 126(3), doi:10.1029/2020jd033881, 2021.
- 521 Hersbach, H., Bell, B., Berrisford, P., Hirahara, S., Horányi, A., Muñoz-Sabater, J.,  
522 Nicolas, J., Peubey, C., Radu, R., Schepers, D., Simmons, A., Soci, C., Abdalla, S.,



- 523 Abellan, X., Balsamo, G., Bechtold, P., Biavati, G., Bidlot, J., Bonavita, M., De Chiara,  
524 G., Dahlgren, P., Dee, D., Diamantakis, M., Dragani, R., Flemming, J., Forbes, R.,  
525 Fuentes, M., Geer, A., Haimberger, L., Healy, S., Hogan, R. J., Hólm, E., Janisková, M.,  
526 Keeley, S., Laloyaux, P., Lopez, P., Lupu, C., Radnoti, G., de Rosnay, P., Rozum, I.,  
527 Vamborg, F., Villaume, S. and Thépaut, J.: The ERA5 global reanalysis, Quarterly  
528 Journal of the Royal Meteorological Society, 146(730), 1999–2049, doi:10.1002/qj.3803,  
529 2020.
- 530 Holton, J. R., Haynes, P. H., McIntyre, M. E., Douglass, A. R., Rood, R. B. and Pfister,  
531 L.: Stratosphere-Troposphere exchange, Reviews of Geophysics, 33(4), 403–439,  
532 doi:10.1029/95rg02097, 1995.
- 533 Iglesias-Suarez, F., Kinnison, D. E., Rap, A., Maycock, A. C., Wild, O. and Young, P. J.:  
534 Key drivers of ozone change and its radiative forcing over the 21st century, Atmospheric  
535 Chemistry and Physics, 18(9), 6121–6139, doi:10.5194/acp-18-6121-2018, 2018.
- 536 Karpechko, A. Yu., Hitchcock, P., Peters, D. H. and Schneidereit, A.: Predictability of  
537 downward propagation of major sudden stratospheric warmings, Quarterly Journal of the  
538 Royal Meteorological Society, 143(704), 1459–1470, doi:10.1002/qj.3017, 2017.
- 539 Kidston, J., Scaife, A. A., Hardiman, S. C., Mitchell, D. M., Butchart, N., Baldwin, M. P.  
540 and Gray, L. J.: Stratospheric influence on tropospheric jet streams, storm tracks and  
541 Surface Weather, Nature Geoscience, 8(6), 433–440, doi:10.1038/ngeo2424, 2015.
- 542 Li, Y., Xia, Y., Xie, F. and Yan, Y.: Influence of stratosphere-troposphere exchange on  
543 long-term trends of surface ozone in CMIP6, Atmospheric Research, 297, 107086,  
544 doi:10.1016/j.atmosres.2023.107086, 2024.



545 Lim, S. S., Vos, T., Flaxman, A. D., Danaei, G., Shibuya, K., Adair-Rohani, H.,  
546 AlMazroa, M. A., Amann, M., Anderson, H. R., Andrews, K. G., Aryee, M., Atkinson,  
547 C., Bacchus, L. J., Bahalim, A. N., Balakrishnan, K., Balmes, J., Barker-Collo, S., Baxter,  
548 A., Bell, M. L., Blore, J. D., Blyth, F., Bonner, C., Borges, G., Bourne, R., Boussinesq,  
549 M., Brauer, M., Brooks, P., Bruce, N. G., Brunekreef, B., Bryan-Hancock, C., Bucello,  
550 C., Buchbinder, R., Bull, F., Burnett, R. T., Byers, T. E., Calabria, B., Carapetis, J.,  
551 Carnahan, E., Chafe, Z., Charlson, F., Chen, H., Chen, J. S., Cheng, A. T.-A., Child, J. C.,  
552 Cohen, A., Colson, K. E., Cowie, B. C., Darby, S., Darling, S., Davis, A., Degenhardt, L.,  
553 Dentener, F., Des Jarlais, D. C., Devries, K., Dherani, M., Ding, E. L., Dorsey, E. R.,  
554 Driscoll, T., Edmond, K., Ali, S. E., Engell, R. E., Erwin, P. J., Fahimi, S., Falder, G.,  
555 Farzadfar, F., Ferrari, A., Finucane, M. M., Flaxman, S., Fowkes, F. G., Freedman, G.,  
556 Freeman, M. K., Gakidou, E., Ghosh, S., Giovannucci, E., Gmel, G., Graham, K.,  
557 Grainger, R., Grant, B., Gunnell, D., Gutierrez, H. R., Hall, W., Hoek, H. W., Hogan, A.,  
558 Hosgood, H. D., Hoy, D., Hu, H., Hubbell, B. J., Hutchings, S. J., Ibeanusi, S. E.,  
559 Jacklyn, G. L., Jasrasaria, R., Jonas, J. B., Kan, H., Kanis, J. A., Kassebaum, N.,  
560 Kawakami, N., Khang, Y.-H., Khatibzadeh, S., Khoo, J.-P., et al.: A comparative risk  
561 assessment of burden of disease and injury attributable to 67 risk factors and risk factor  
562 clusters in 21 regions, 1990–2010: A systematic analysis for the global burden of disease  
563 study 2010, *The Lancet*, 380(9859), 2224–2260, doi:10.1016/s0140-6736(12)61766-8,  
564 2012.

565 Limpasuvan, V., Thompson, D. W. and Hartmann, D. L.: The life cycle of the Northern  
566 Hemisphere sudden stratospheric warmings, *Journal of Climate*, 17(13), 2584–2596,  
567 doi:10.1175/1520-0442(2004)017<2584:tlcotn>2.0.co;2, 2004.



- 568 Lin, Y., Jiang, F., Zhao, J., Zhu, G., He, X., Ma, X., Li, S., Sabel, C. E. and Wang, H.:  
569 Impacts of O<sub>3</sub> on premature mortality and crop yield loss across China, *Atmospheric*  
570 *Environment*, 194, 41–47, doi:10.1016/j.atmosenv.2018.09.024, 2018.
- 571 Lu, Q., Rao, J., Shi, C., Guo, D., Fu, G., Wang, J. and Liang, Z.: Possible influence of  
572 sudden stratospheric warmings on the atmospheric environment in the Beijing–Tianjin–  
573 Hebei region, *Atmospheric Chemistry and Physics*, 22(19), 13087–13102,  
574 doi:10.5194/acp-22-13087-2022, 2022.
- 575 Lu, Q., Rao, J., Shi, C., Ren, R., Liu, Y. and Liu, S.: Stratosphere-troposphere coupling  
576 during stratospheric extremes in the 2022/23 winter, *Weather and Climate Extremes*, 42,  
577 100627, doi:10.1016/j.wace.2023.100627, 2023.
- 578 Ma, X., Huang, J., Hegglin, M., Joeckel, P. and Zhao, T.: Causes of growing middle-  
579 upper tropospheric ozone over the Northwest Pacific Region, doi:10.5194/egusphere-  
580 2023-2411, 2024.
- 581 Manney, G. L., Lawrence, Z. D., Santee, M. L., Livesey, N. J., Lambert, A. and Pitts, M.  
582 C.: Polar Processing in a split vortex: Arctic ozone loss in early Winter 2012/2013,  
583 *Atmospheric Chemistry and Physics*, 15(10), 5381–5403, doi:10.5194/acp-15-5381-2015,  
584 2015.
- 585 McIntyre, M. E. and Palmer, T. N.: Breaking planetary waves in the stratosphere, *Nature*,  
586 305(5935), 593–600, doi:10.1038/305593a0, 1983.
- 587 McIntyre, M. E.: How well do we understand the dynamics of stratospheric warmings?,  
588 *Journal of the Meteorological Society of Japan. Ser. II*, 60(1), 37–65,  
589 doi:10.2151/jmsj1965.60.1\_37, 1982.



- 590 Mitchell, D. M., Gray, L. J., Anstey, J., Baldwin, M. P. and Charlton-Perez, A. J.: The  
591 influence of stratospheric vortex displacements and splits on surface climate, *Journal of*  
592 *Climate*, 26(8), 2668–2682, doi:10.1175/jcli-d-12-00030.1, 2013.
- 593 Myhre, G., Jonson, J. E., Bartnicki, J., Stordal, F. and Shine, K. P.: Role of spatial and  
594 temporal variations in the computation of radiative forcing due to sulphate aerosols: A  
595 regional study, *Quarterly Journal of the Royal Meteorological Society*, 128(581), 973–  
596 989, doi:10.1256/0035900021643610, 2002.
- 597 Myhre, G., Shine, K. P., Rädcl, G., Gauss, M., Isaksen, I. S. A., Tang, Q., Prather, M. J.,  
598 Williams, J. E., van Velthoven, P., Dessens, O., Koffi, B., Szopa, S., Hoor, P., Grewe, V.,  
599 Borken-Kleefeld, J., Berntsen, T. K. and Fuglestedt, J. S.: Radiative forcing due to  
600 changes in ozone and methane caused by the transport sector, *Atmospheric Environment*,  
601 45(2), 387–394, doi:10.1016/j.atmosenv.2010.10.001, 2011.
- 602 Ou-Yang, C.-F., Babu, S. R., Lee, J.-R., Yen, M.-C., Griffith, S. M., Lin, C.-C., Chang,  
603 S.-C. and Lin, N.-H.: Detection of stratospheric intrusion events and their role in ozone  
604 enhancement at a mountain background site in sub-tropical East Asia, *Atmospheric*  
605 *Environment*, 268, 118779, doi:10.1016/j.atmosenv.2021.118779, 2022.
- 606 Rathore, A., Gopikrishnan, G. S. and Kuttippurath, J.: Changes in tropospheric ozone  
607 over India: Variability, long-term trends and climate forcing, *Atmospheric Environment*,  
608 309, 119959, doi:10.1016/j.atmosenv.2023.119959, 2023.
- 609 Roy, C., Ravishankara, A. R., Newman, P. A., David, L. M., Fadnavis, S., Rathod, S. D.,  
610 Lait, L., Krishnan, R., Clark, H. and Sauvage, B.: Estimation of stratospheric intrusions  
611 during Indian Cyclones, *Journal of Geophysical Research: Atmospheres*, 128(3),  
612 doi:10.1029/2022jd037519, 2023.



- 613 Scheffler, J., Ayarzagüena, B., Orsolini, Y. J. and Langematz, U.: Elevated stratopause  
614 events in the current and a future climate: A chemistry-climate model study, *Journal of*  
615 *Atmospheric and Solar-Terrestrial Physics*, 227, 105804,  
616 doi:10.1016/j.jastp.2021.105804, 2022.
- 617 Schimanke, S., Spanghel, T., Huebener, H. and Cubasch, U.: Variability and trends of  
618 major stratospheric warmings in simulations under constant and increasing GHG  
619 concentrations, *Climate Dynamics*, 40(7–8), 1733–1747, doi:10.1007/s00382-012-1530-  
620 x, 2012.
- 621 Shell, K. M., Kiehl, J. T. and Shields, C. A.: Using the radiative kernel technique to  
622 calculate climate feedbacks in NCAR’s community atmospheric model, *Journal of*  
623 *Climate*, 21(10), 2269–2282, doi:10.1175/2007jcli2044.1, 2008.
- 624 Shi, G., Krochin, W., Sauvageat, E. and Stober, G.: Ozone anomalies over the polar  
625 regions during stratospheric warming events, *Atmospheric Chemistry and Physics*,  
626 24(17), 10187–10207, doi:10.5194/acp-24-10187-2024, 2024.
- 627 Sigmond, M., Scinocca, J. F., Kharin, V. V. and Shepherd, T. G.: Enhanced seasonal  
628 forecast skill following stratospheric sudden warmings, *Nature Geoscience*, 6(2), 98–102,  
629 doi:10.1038/ngeo1698, 2013.
- 630 Silva, R. A., West, J. J., Zhang, Y., Anenberg, S. C., Lamarque, J.-F., Shindell, D. T.,  
631 Collins, W. J., Dalsoren, S., Faluvegi, G., Folberth, G., Horowitz, L. W., Nagashima, T.,  
632 Naik, V., Rumbold, S., Skeie, R., Sudo, K., Takemura, T., Bergmann, D., Cameron-  
633 Smith, P., Cionni, I., Doherty, R. M., Eyring, V., Josse, B., MacKenzie, I. A., Plummer,  
634 D., Righi, M., Stevenson, D. S., Strode, S., Szopa, S. and Zeng, G.: Global premature  
635 mortality due to anthropogenic outdoor air pollution and the contribution of past climate



- 636 change, *Environmental Research Letters*, 8(3), 034005, doi:10.1088/1748-  
637 9326/8/3/034005, 2013.
- 638 Skeie, R. B., Myhre, G., Hodnebrog, Ø., Cameron-Smith, P. J., Deushi, M., Hegglin, M.  
639 I., Horowitz, L. W., Kramer, R. J., Michou, M., Mills, M. J., Olivié, D. J., Connor, F. M.,  
640 Paynter, D., Samset, B. H., Sellar, A., Shindell, D., Takemura, T., Tilmes, S. and Wu, T.:  
641 Historical total ozone radiative forcing derived from CMIP6 simulations, *npj Climate and*  
642 *Atmospheric Science*, 3(1), doi:10.1038/s41612-020-00131-0, 2020.
- 643 Stamnes, K., Tsay, S.-C., Wiscombe, W. and Jayaweera, K.: Numerically stable  
644 algorithm for discrete-ordinate-method radiative transfer in multiple scattering and  
645 emitting layered media, *Applied Optics*, 27(12), 2502, doi:10.1364/ao.27.002502, 1988.
- 646 Veenus, V., Das, S. S. and David, L. M.: Ozone changes due to sudden stratospheric  
647 warming-induced variations in the intensity of Brewer-Dobson Circulation: A composite  
648 analysis using observations and chemical-transport model, *Geophysical Research Letters*,  
649 50(13), doi:10.1029/2023gl1103353, 2023.
- 650 Wang, H., Lu, X., Jacob, D. J., Cooper, O. R., Chang, K.-L., Li, K., Gao, M., Liu, Y.,  
651 Sheng, B., Wu, K., Wu, T., Zhang, J., Sauvage, B., Nédélec, P., Blot, R. and Fan, S.:  
652 Global tropospheric ozone trends, attributions, and radiative impacts in 1995–2017: An  
653 integrated analysis using aircraft (IAGOS) observations, ozonesonde, and multi-decadal  
654 chemical model simulations, *Atmospheric Chemistry and Physics*, 22(20), 13753–13782,  
655 doi:10.5194/acp-22-13753-2022, 2022.
- 656 Wang, M. and Fu, Q.: Stratosphere-troposphere exchange of Air Masses and ozone  
657 concentrations based on reanalyses and observations, *Journal of Geophysical Research:*  
658 *Atmospheres*, 126(18), doi:10.1029/2021jd035159, 2021.



- 659      Waugh, D. W. and Polvani, L. M.: Climatology of intrusions into the tropical upper  
660      troposphere, *Geophysical Research Letters*, 27(23), 3857–3860,  
661      doi:10.1029/2000gl012250, 2000.
- 662      Williams, R. S., Hegglin, M. I., Jöckel, P., Garny, H. and Shine, K. P.: Air quality and  
663      radiative impacts of downward-propagating sudden stratospheric warmings (ssws),  
664      *Atmospheric Chemistry and Physics*, 24(2), 1389–1413, doi:10.5194/acp-24-1389-2024,  
665      2024.
- 666      Williams, R. S., Hegglin, M. I., Kerridge, B. J., Jöckel, P., Latter, B. G. and Plummer, D.  
667      A.: Characterising the seasonal and geographical variability in tropospheric ozone,  
668      stratospheric influence and recent changes, *Atmospheric Chemistry and Physics*, 19(6),  
669      3589–3620, doi:10.5194/acp-19-3589-2019, 2019.
- 670      Xia, Y., Xie, F. and Lu, X.: Enhancement of Arctic surface ozone during the 2020–2021  
671      winter associated with the sudden stratospheric warming, *Environmental Research*  
672      *Letters*, 18(2), 024003, doi:10.1088/1748-9326/acaee0, 2023.
- 673      Yin, X., Rupakheti, D., Zhang, G., Luo, J., Kang, S., de Foy, B., Yang, J., Ji, Z., Cong, Z.,  
674      Rupakheti, M., Li, P., Hu, Y. and Zhang, Q.: Surface ozone over the Tibetan Plateau  
675      controlled by stratospheric intrusion, *Atmospheric Chemistry and Physics*, 23(17),  
676      10137–10143, doi:10.5194/acp-23-10137-2023, 2023.
- 677      Ziemke, J. R., Chandra, S. and Bhartia, P. K.: “cloud slicing”: A new technique to derive  
678      upper tropospheric ozone from satellite measurements, *Journal of Geophysical Research:*  
679      *Atmospheres*, 106(D9), 9853–9867, doi:10.1029/2000jd900768, 2001.